

# New texture signatures and their use in rotation invariant texture classification

Jianguo Zhang, Tieniu Tan

► **To cite this version:**

Jianguo Zhang, Tieniu Tan. New texture signatures and their use in rotation invariant texture classification. Proceedings of Texture 2002 (The 2nd international workshop on texture analysis and synthesis with ECCV 2002), Jun 2002, Copenhagen, Denmark. pp.157–162, 2002. <inria-00548245>

**HAL Id: inria-00548245**

**<https://hal.inria.fr/inria-00548245>**

Submitted on 20 Dec 2010

**HAL** is a multi-disciplinary open access archive for the deposit and dissemination of scientific research documents, whether they are published or not. The documents may come from teaching and research institutions in France or abroad, or from public or private research centers.

L'archive ouverte pluridisciplinaire **HAL**, est destinée au dépôt et à la diffusion de documents scientifiques de niveau recherche, publiés ou non, émanant des établissements d'enseignement et de recherche français ou étrangers, des laboratoires publics ou privés.

# New Texture Signatures and Their Use in Rotation Invariant Texture Classification<sup>1</sup>

Jianguo Zhang, Tieniu Tan

National Lab of Pattern Recognition (NLPR), Institute of Automation, Chinese Academy of Sciences,  
Beijing 100080, P. R. China Email: {jgzhang, tnt}@nlpr.ia.ac.cn

**Abstract--** In this paper, we present a theoretically and computationally simple but efficient approach for rotation invariant texture classification. This method is based on new texture signatures extracted from spectrum. Rotation invariant texture features are obtained based on the extension of the derived signatures. The features are tested with 1000 randomly rotated samples of 20 Brodatz texture classes. Comparative study results show that our method is highly efficient in rotation invariant texture classification.

## 1. INTRODUCTION

Texture analysis is a fundamental issue in image processing, computer vision and their applications, such as object recognition, remote sensing, content-based image retrieval and so on. It has been an active research topic for more than three decades. Numerous methods have been proposed in the open literature [1][2][3]. The majority of existing methods make the explicit or implicit assumption that texture images are acquired from the same viewpoint (e.g. the same scale and orientation). However in many practical applications such as content-based viewpoint image retrieval, images obtained are often subject to geometric distortions including translation, rotation, scaling and skew. Furthermore, given a texture image, according to our own experience or cognitive theory, no matter how it changes under geometric transform, A geometrically transformed texture is always perceived as the same textures by human observer. So texture features should ideally be invariant to viewpoint. It has been received more and more attentions [12]. Recent surveys of existing work on the important subject may be found in [7][8].

In this paper, we propose a new method for rotation invariant texture feature extraction. Based on rotation spectrum representation of a texture image, a signature distribution function is obtained. By applying the Fourier expansion on this function, rotation invariance is achieved. We examine the usefulness of these proposed features with a database of 1000 randomly rotated textures. Extensive comparative study with Gabor features shows that the proposed algorithm is highly efficient in invariant texture classification.

## 2. ROTATION INVARIANT TEXTURE SIGNATURES

In this section, we propose an algorithm of computing the new texture signatures, evaluate its performance in capturing the texture properties and further develop it to achieve rotation invariance.

### 2.1 Projection

Let  $f(x, y)$  be the original texture image. Define the projection of  $f(x, y)$  onto a line  $l$  at angle  $\theta$  with the x-axis as follows:

$$p(l/\theta) = \int_{-\infty}^{+\infty} f(\vec{z} \cdot \vec{\alpha}, \vec{z} \cdot \vec{\beta}) d(\vec{z} \cdot \vec{\beta})$$

where  $\vec{z} = [x \ y]$ ,  $\vec{\alpha} = \begin{bmatrix} \cos(\theta) \\ \sin(\theta) \end{bmatrix}$ ,  $\vec{\beta} = \begin{bmatrix} -\sin(\theta) \\ \cos(\theta) \end{bmatrix}$  (1)

In the special case of  $\theta = 0$ , we obtain the vertical projection onto the x-axis:

$$p(l/\theta = 0) = \int_{-\infty}^{+\infty} f(x, y) dy$$
 (2)

The projection function can capture the regularity of textures at different orientations. This can be illustrated in Figure 1 (In this figure,  $\theta = 0$ ). From this figure we can see that if texture images such as D001 are periodic along the direction at a certain angle, the projection function at this orientation tends to be quite regular. On the other hand if textures such as D019 are random at this orientation, so does its projection function at this angle. This observation indicates the usefulness of the projection function in measuring texture properties. It is obvious that for a given texture image, the texture regularity often varies with change of orientation. The changes of this regularity can be captured by the projection on lines at all orientations (See Equation (1)).

The following shows that the projection of  $f(x, y)$  onto a line at angle can be evaluated by its Fourier version at the line at  $\theta$ .

Let  $f_r(x_r, y_r)$  be the rotated version of  $f(x, y)$ . Then the relationship of these two images is formulated as follows:

$$f_r(x_r, y_r) = f(x, y); \begin{bmatrix} x_r \\ y_r \end{bmatrix} = \begin{bmatrix} R_{11} & R_{12} \\ R_{21} & R_{22} \end{bmatrix} \begin{bmatrix} x \\ y \end{bmatrix}$$
 (3)

<sup>1</sup> this work is funded by research grants from the NSFC (Grant No. 69825105 and 69790080) and the Chinese Academy of Sciences

Let matrix  $R$  denote the orthogonal matrix  $\begin{bmatrix} R_{11} & R_{12} \\ R_{21} & R_{22} \end{bmatrix}$ .

It is well known that when the original texture rotated by an angle, the frequency spectrum is also rotated by the same angle (this is the rotation property of the Fourier transform). The relationship of the spectra of the original and rotated image is described as follows:

$$|F_r(u_r, v_r)| = |F(u, v)| \begin{pmatrix} u_r \\ v_r \end{pmatrix} = R_T^{-1} \begin{pmatrix} u \\ v \end{pmatrix} \quad (4)$$

where  $F(u, v)$  is the Fourier transform of the original texture  $f(x, y)$ ,  $F_r(u_r, v_r)$  that of  $f_r(x_r, y_r)$ .  $R_T^{-1}$  is the inverse of the transpose of matrix  $R$ .

The one-dimensional Fourier transform of Equation (2) is

$$P(u) = \int_{-\infty}^{+\infty} \int_{-\infty}^{+\infty} f(x, y) dy e^{-j2\pi ux} dx \quad (5)$$

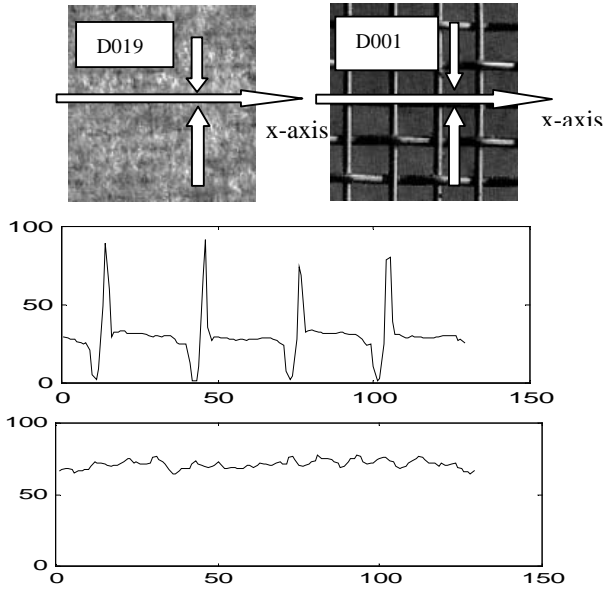


Figure 1 Illustration of properties of the projection in measuring texture properties.

The first row is the original Brodatz textures D019 and D001  
The second row is the projection of D001 onto x-axis (regular)

$P(u)$  can also be written in another form

$$P(u) = \int_{-\infty}^{+\infty} \int_{-\infty}^{+\infty} f(x, y) e^{-j2\pi(u x + 0 y)} dx dy = F(u, 0) \quad (6)$$

Equation (6) implies that the projection of  $f(x, y)$  onto the x-axis is  $F(u, v)$  evaluated along the u-axis. This is the direct result of the separability of Fourier transform. More generally, combining with the rotation property, the one-dimensional Fourier transform of  $f(x, y)$  projected onto a line at angle  $\theta$  with the x-axis is just  $F(u, v)$  evaluated along the line at angle  $\theta$  with the  $u$ -axis. That is Equation (1) can be evaluated by  $F(u, v)$  alternatively. This produces a

feasible way of the projection function analysis.

## 2.2 Rotation invariant texture signatures

Let  $\rho = \sqrt{u^2 + v^2}$ ,  $\theta = \arctg(u/v)$ ,  $F(\rho, \theta)$  be the Fourier transform of the projection of  $f(x, y)$  onto a line at

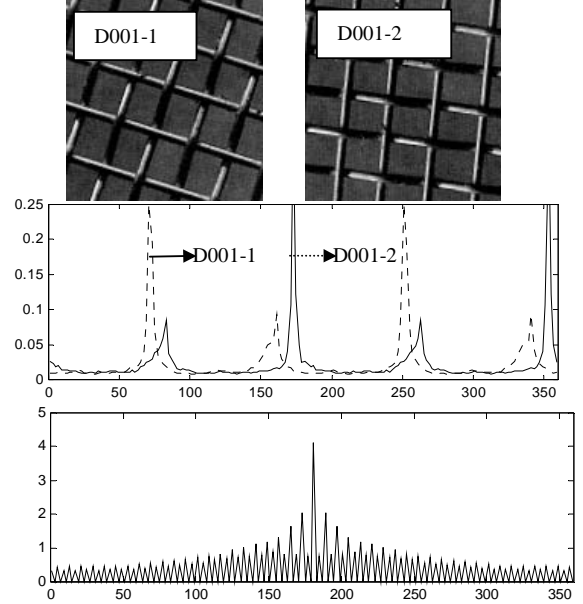


Figure 2 Illustration of the rotation affection on signatures

The first row is the two rotated examples of texture D001

The second row is the corresponding signatures

The third row is the Fourier magnitude of the tow signatures

angle  $\theta$  and  $F_r(\rho_r, \theta_r)$  that of the Projection of  $f_r(x_r, y_r)$  onto a line at angle  $\theta_r$ . Their relationship can be represented as follows:

$$F_r(\rho_r, \theta_r) = F(\rho, \theta) \quad (7)$$

Since the frequency distribution (here we consider spectrum magnitude as the probability of the corresponding frequency) can give a description of texture periodicity, we calculate the central moment of Equation (7) as follows:

$$c_r(\theta_r) = \int (\rho_r - \bar{\rho}_r) F_r(\rho_r, \theta_r) d\rho_r$$

$$c(\theta) = \int (\rho - \bar{\rho}) F(\rho, \theta) d\rho \quad (8)$$

where  $\bar{\rho}$  and  $\bar{\rho}_r$  are the mean value of  $\rho$  and  $\rho_r$ .  $c(\theta)$  measures the periodicity of texture regularity. Notice that the power spectrum provides a measurement of the amplitude of texture regularity. Thus we take it into account and compute the spectrum signatures at angle  $\theta$  and  $\theta_r$  ( $\theta_r = \theta + \Delta\theta$ ) as follows:

$$T(\theta_r) = c_r(\theta_r) \int F_r(\rho_r, \theta_r) d\rho_r$$

$$= c(\theta) \int F(\rho, \theta) d\rho = T(\theta) \quad (9)$$

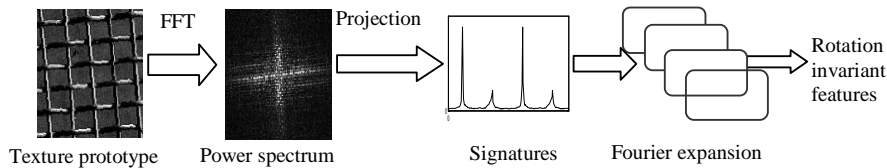


Figure 3 Schematic diagram of the rotation invariant texture feature extraction algorithm

Such that we have obtained the orientation spectrum signatures  $T(\theta)$ . It is obvious that the texture signature is rotation dependent and it is a periodic function of  $\theta$  with a period of  $2\pi$ . Assume  $T(\theta)$  is computed from  $f(x, y)$  and  $T(\theta_r)$  from  $f_r(x_r, y_r)$  rotated by  $\Delta\theta$  from  $f(x, y)$ . It is not difficult to see that  $T(\theta) = T(\theta_r)$  if  $\theta_r - \theta = \Delta\theta$ . This implies that a rotation of the input image  $f(x, y)$  by  $\Delta\theta$  is equivalent to a translation of its spectrum signatures by the same amount along the orientation axis. The relationship between  $T(\theta)$  and  $T(\theta_r)$  is illustrated in Figure 2. The translation between the two plots is evident, however they share almost the same Fourier magnitude response. Since that the Fourier magnitude is invariant to translation, thus the Fourier expansion of  $T(\theta)$  provides a set of rotation invariant features for the input image  $f(x, y)$ . Figure 3 shows the overall scheme of the extraction of the rotation invariant texture features. It consists of three major steps as discussed above.

### 3. EXPERIMENTAL RESULTS

In order to test the efficacy of the proposed features for rotation invariant texture analysis, we carry out the experiment on 20 structured texture images selected from the Brodatz album as illustrated in Figure 4 (note that if textures are isotropic or randomness, any texture descriptors will be invariant to rotation [9]). Each texture image of size 512x512 is randomly rotated into 15 versions, from which subimages of size 128x128 are extracted. Thus a database of 1000 images is constructed for this experiment. A database of 140 (7 for each texture class) is used for training and the remaining (860 images, 43 for each texture) for testing. Texture signature distribution  $T(\theta)$  is extracted from each image, and its Fourier amplitude is used as the rotation invariant texture features. The first 7 magnitudes are selected to construct a 7-dimensional-feature vector for use in rotation invariant texture classification. Euclidean distance is calculated to measure the similarity between textures.

The K-nearest neighborhood classifier is employed. An average correct recognition rate of 98.95% is obtained. Classification results of each texture class are shown in Figure 5. This clearly shows the promising efficacy of the proposed features for rotation invariant texture classification.

In our previous work, we have proposed rotation invariant texture descriptors [4][5][9] and conducted a comparative study of four methods on invariant texture classification

(Gabor features, HMM, an edge attribute processing model, and the circular simultaneous autoregressive model)[5]. Details may be found in these papers. In this paper, we do not have to repeat these comparisons. We only compare our method with rotation invariant Gabor features which have been shown to be most effective in [5][6]. We do this to further highlight the performance of the new proposed feature in rotation invariant texture classification. We carry out this comparative study under the same condition mentioned above. An average classification accuracy of 98.90% is obtained by using Gabor features. Our study indicates that the method achieves almost the same classification results as Gabor features and human shown in Figure 6. However, the computational cost of the Gabor method is much higher than the proposed algorithm. Furthermore, it should be pointed out that rotation invariant Gabor features suffers from the sampling problem of Gabor channel. We conduct this study on the same database as described above by changing the sampling interval between Gabor channels. The results shown in Figure 7 indicate that the performance of Gabor features deteriorates as the sampling interval between Gabor channels becomes larger (or the number of Gabor channels decreases). To achieve a higher accuracy, the interval of the Gabor channel must be smaller. This will increase the computation cost and complexity (note that the amount of overlap between Gabor channels will also increase in the spatial and frequency domain [11]). From this viewpoint, the proposed new algorithm is of less computational complexity.

### 4 CONCLUSIONS AND FUTURE WORK

We have proposed a theoretically and computationally simple algorithm of extracting texture signatures that can capture texture properties. The new signature is computed in the spectrum domain. It has been developed to obtain rotation invariant texture features. The invariant features are obtained based on the Fourier expansion of the signatures. Our comparative study shows its high effectiveness in rotation invariant texture classification. Further research should include its robustness to image noise, their use in rotation invariant image retrieval and affine invariant texture classification.

### REFERENCES

- [1] M. Tuceryan and A.K. Jain, Texture Analysis, in Handbook of Pattern Recognition and Computer Vision (C. H. Chen, et. al., Eds), 1993, pp.235-276.
- [2] A.R. Rao, Taxonomy for Texture Description and Identification. Springer Verlag: Berlin, 1990.

[3] F. Tomita, and S. Tsuji, Computer Analysis of Visual Textures, Hingham, MA: Kluwer Academic, 1990

[4] S.R. Fountain, T.N. Tan, "Efficient Rotation Invariant Texture Features for Content-based Image Retrieval". *Pattern recognition*, Vol. 31, No. 11 1998, pp1725-1732.

[5] S.R Fountain, T.N. Tan, " a Comparative Study of Rotation Invariant Classification and Retrieval of Texture images. *Procs. of BMVC*, Vol. 1, pp. 266-275. 1998

[6] R. Porter Robust rotation invariant texture classification: wavelet, Gabor filter, and GMRF based schemes, *IEE Proc. -Vis. Image Signal Process.*, Vol. 144, No. 3, June, 1997.

[7] T.N. Tan, "Geometric transform invariant texture analysis," *SPIE*. Vol. 2488, pp475-485, 1995.

[8] J.G. Zhang and T.N. Tan, "Brief review of invariant texture analysis methods," *Pattern Recognition*, Vol. 35/3, pp.735-747, 2002.

[9] T.N.Tan, "Rotation invariant texture features and their use in automatic script identification," *IEEE Trans. Pattern Analysis and Machine Intelligence* Vol.20, No.7, pp. 751-756, July 1998.

[10] P. Brodatz, Textures: A Photographic Album for Artist and Designer. Dover, New York (1966).

[11] A.K. Jain, F. Farrokhnia "Unsupervised texture segmentation using Gabor filters", *Pattern Recognition*, Vol. 24, No. 12, pp.1167-1186, 1991.

[12] M. Pietikainen, T. Ojala, Z. Xu, Rotation-Invariant texture classification using feature distributions, *Pattern Recognition* 33 (2000) pp. 975-985

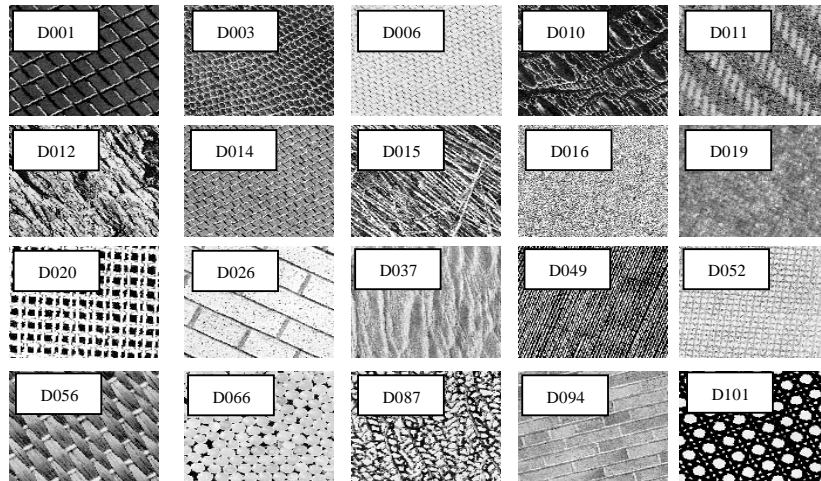


Figure 4 20 textures from Brodatz database used for rotation invariant texture classification

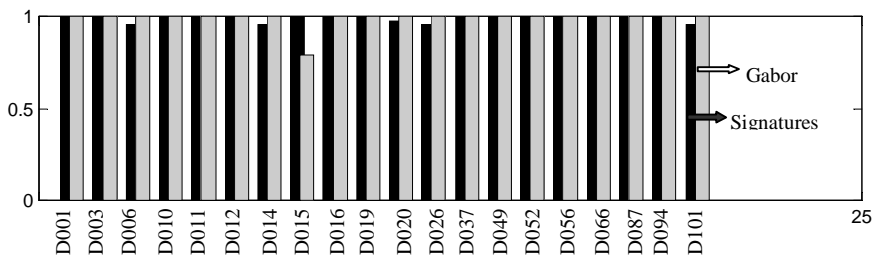


Figure5 Classification results of rotation invariant Gabor features and signatures

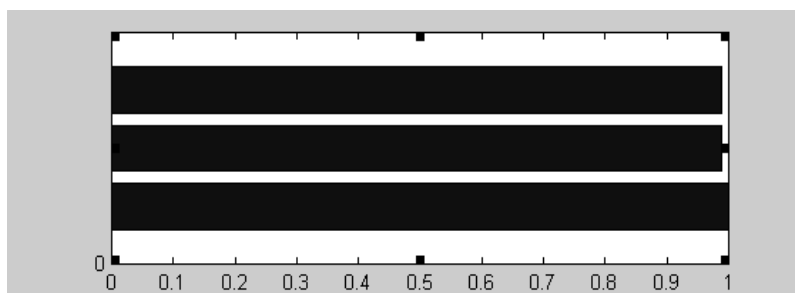


Figure 6 Comparison of performance of Gabor, Signature, and Human for rotation invariant texture classification

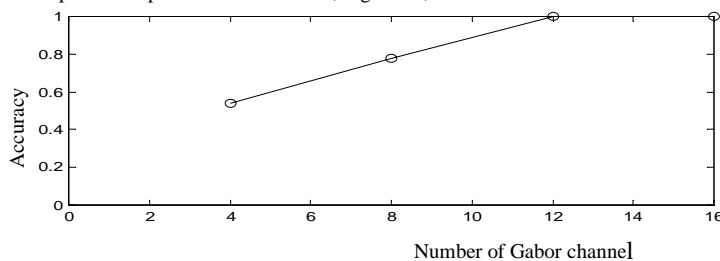


Figure 7 Performance of the rotation invariant Gabor features vs. the number of Gabor channels